

Epipolar Consistency Guided Beam Hardening Reduction - ECC²

Tobias Würfl^{*}, Nicole Maaß[†], Frank Dennerlein[†], Xiaolin Huang^{*}, Andreas K. Maier^{*}

^{*}Pattern Recognition Lab, Department of Computer Science,

Friedrich-Alexander-Universität Erlangen-Nürnberg, Erlangen, Germany,

[†]Siemens Healthcare GmbH, Erlangen, Germany

Abstract—Beam hardening is a problem arising in every computed tomography scan with a conventional X-ray tube. We describe a new calibration-free, computationally efficient algorithm for mono-material beam hardening reduction. It is based on optimization of the Epipolar consistency condition on computed tomography raw data. The efficiency of our approach is achieved by formulating the optimization problem directly on the Radon intermediate function conventionally used by these consistency conditions. We thus avoid recalculating the intermediate function and can solve a homogeneous least squares optimization problem. We regularize the ill-posed homogeneous problem by introduction of a regularizer which keeps the dynamic range of the projection data constant. The resulting constrained problem can be solved in closed form. To demonstrate the effectiveness of our approach we apply our method to simulation experiments. We additionally provide experimental insight to the robustness of our algorithm to image noise, geometrical noise and truncation. As a last experiment we apply our method to real data.

I. INTRODUCTION

Beam hardening is a common problem in X-ray computed tomography which is caused by the polychromatic spectrum of conventional X-ray sources combined with the energy dependence of the linear attenuation coefficient. It causes severe image artifacts such as cupping, streaks and negative regions in reconstructions [1].

Many different prior approaches exist to reduce the effect of beam hardening. They can be roughly divided in approaches reducing it during acquisition, like optimization of the X-ray spectrum, or approaches reducing the effect with algorithms. The algorithmic approaches either use a mono-material or a multi-material model. A well-known mono-material approach was presented by Kachelrieß et al. [2]. They assume a polynomial model for the line integral measurements and calculate its parameters from a calibration scan of a homogeneous phantom of a known material.

Some multi-material methods decompose the different materials in a preliminary reconstruction [3] and estimate different parameters for the mono-material images. A computationally efficient approach doing this has been presented by Wu et al. [4].

Beam hardening will also introduce inconsistencies into the projection data which will be reflected by consistency

conditions used to reduce geometric misalignment. Three well-known formulations of consistency conditions are the Helgason-Ludwig [5], the Fourier [6] and the Epipolar consistency condition [7]. The Epipolar consistency condition is directly applicable to cone beam projection data.

However the introduced inconsistency also presents an opportunity to reduce beam hardening using consistency conditions. A restoration model can be adopted and its parameters optimized by minimization of the inconsistency. Different methods using the Helgason-Ludwig consistency condition have been presented e.g. by Tang et al. [8]. An approach by Abdurahman et al. uses the Epipolar consistency condition in cone beam geometry [9]. A big advantage of consistency-based methods is, that they provide an optimization target directly from redundancies in the measured raw data. This way no prior knowledge about the X-ray source or the materials of the object is needed. A common drawback of these methods is their computational demand.

Using the Epipolar consistency condition, we derive a computationally efficient mono-material beam hardening reduction algorithm. We choose the popular polynomial model and estimate its parameters by optimization of consistency. The key difference to the method by Abdurahman et al. is the formulation of the optimization problem in the domain of the intermediate function, which enables to keep it constant during optimization. The main idea for our formulation combines the Epipolar consistency condition (ECC) and the linearity of the Radon transform, similar to empirical cupping correction (ECC) [2], which leads us to the acronym ECC². We show that our formulation leads to an overconstrained homogeneous system of linear equations allowing an efficient solution.

II. METHODOLOGY

In Sect. II-A we introduce the Epipolar consistency condition as presented by Aichert et al. [7]. We then formulate our optimization problem on the intermediate function in Sect. II-B. We subsequently show how this problem can be solved uniquely and efficiently.

A. Epipolar Consistency Condition

The Epipolar consistency condition emerges out of Grangeats theorem [10], which establishes a fundamental

relation between the derivatives in normal direction of the 3D Radon transform and the X-ray transform. This has been presented by Debbeler et al. [11], before being introduced as Epipolar consistency condition by Aichert et al.[7]. Aichert et al. state in equation (31) of [7] that the derivatives in normal direction $\frac{d}{dn}$ of the Epipolar plane of the 3D Radon transform, denoted by $\frac{d}{dn}\rho_R(\mathbf{E})$ approximately equal the derivatives in spatial direction $\frac{d}{dt}$ of line integrals along the detector $\frac{d}{dt}\rho_{\mathbf{I}}(\mathbf{l})$, where \mathbf{l} denotes the intersection of the plane \mathbf{E} with the detector:

$$\frac{d}{dt}\rho_{\mathbf{I}_0}(\mathbf{l}_0) \approx \frac{d}{dn}\rho_R(\mathbf{E}) \approx \frac{d}{dt}\rho_{\mathbf{I}_1}(\mathbf{l}_1). \quad (1)$$

Here \mathbf{l}_0 and \mathbf{l}_1 denote a corresponding pair of Epipolar lines with the indices distinguishing the different lines dependant on their detector position. The index R of ρ_R here distinguishes the 3D Radon transform of the object from the Radon transform of the projection images $\rho_{\mathbf{I}_0}$ and $\rho_{\mathbf{I}_1}$. They proceed by formulating a metric between two projection images as:

$$\hat{M}_0^1 = \int_{-\frac{\pi}{2}}^{\frac{\pi}{2}} \left(\frac{d}{dt}\rho_{\mathbf{I}_0}(\mathbf{l}_0) - \frac{d}{dt}\rho_{\mathbf{I}_1}(\mathbf{l}_1) \right)^2 d\alpha, \quad (2)$$

where α is an angle between a reference plane and other Epipolar planes. An important acceleration strategy in their formulation is to compute a discretization of line integrals of the projections by calculating their Radon transforms. This allows one to replace the integration step in the evaluation of the consistency condition by a sampling and therefore greatly speeds up the process.

B. Epipolar Consistency Guided Beam Hardening Reduction

The conceptual goal of a beam hardening reduction algorithm based on this consistency is to optimize the parameters \mathbf{w} of some beam hardening reduction model denoted by f :

$$\frac{d}{dt}\rho_{f(\mathbf{I}_0, \mathbf{w})}(\mathbf{l}_0) \approx \frac{d}{dt}\rho_{f(\mathbf{I}_1, \mathbf{w})}(\mathbf{l}_1). \quad (3)$$

Two key problems can be derived from this equation:

- The precomputed line integrals are only valid for a single choice of \mathbf{w} and
- a solution can only be determined up to scale.

We use the well-known polynomial model[2]. An advantage of such a non-linear basis series model is, that despite being non-linear, it is linear in its parameters. Plugging this model into equation 3 we receive

$$\frac{d}{dt}\rho\left(\sum_{n=1}^N w_n \mathbf{I}_0^n\right)(\mathbf{l}_0) \approx \frac{d}{dt}\rho\left(\sum_{n=1}^N w_n \mathbf{I}_1^n\right)(\mathbf{l}_1). \quad (4)$$

Here \mathbf{I}^n denotes transforming every pixel of projection \mathbf{I} independently to its n -th power. Because of the linearity of the Radon transform and the derivative operator we can reuse the idea of empirical cupping correction [2] and rewrite equation 4 to:

$$\sum_{n=1}^N w_n \left(\frac{d}{dt}\rho_{\mathbf{I}_0^n}(\mathbf{l}_0) \right) \approx \sum_{n=1}^N w_n \left(\frac{d}{dt}\rho_{\mathbf{I}_1^n}(\mathbf{l}_1) \right). \quad (5)$$

This solves key problem (a), because the powers of the intermediate functions $\frac{d}{dt}\rho_{\mathbf{I}^n}$ stay constant during optimization. We can now optimize for consistency:

$$\min \left(\sum_{n=1}^N w_n a_n \right)^2, \quad a_n = \left(\frac{d}{dt}\rho_{\mathbf{I}_0^n}(\mathbf{l}_0) - \frac{d}{dt}\rho_{\mathbf{I}_1^n}(\mathbf{l}_1) \right). \quad (6)$$

Since we want to solve this problem for many different projections and epipolar planes, there are M measurements a_{mn} , producing a homogeneous overdetermined system of linear equations, which can therefore only be solved in a least squares sense and up to scale. A typical solution for the scaling is to restrict the ℓ_2 -norm of \mathbf{w} to $\|\mathbf{w}\|_2^2 = 1$. However this rescales the data in an arbitrary way. Our proposed solution is to rescale \mathbf{w} requiring

$$\beta = \sum_{n=1}^N w_n b^n = \mathbf{w}^T \mathbf{b} \quad (7)$$

for an arbitrary line integral b of the projections and β , the value b will take on after beam hardening reduction. Here \mathbf{b}^T denotes the vector: $[b^1 \ \dots \ b^N]$. This problem can then be stated as:

$$\min(\|\mathbf{A}\mathbf{w}\|_2^2) \quad \text{s.t.} : \mathbf{w}^T \mathbf{b} = \beta \quad (8)$$

Where \mathbf{A} denotes a measurement matrix:

$$\begin{bmatrix} a_{01} & \dots & a_{0N} \\ \vdots & \ddots & \vdots \\ a_{M1} & \dots & a_{MN} \end{bmatrix}.$$

The M rows of the matrix represent different consistency equations involving N coefficients w_n of the polynomial which have to hold simultaneously. The Lagrangian function of this problem is:

$$L(\mathbf{w}, \lambda) = \mathbf{w}^T \mathbf{A}^T \mathbf{A} \mathbf{w} + \lambda(\beta - \mathbf{w}^T \mathbf{b}). \quad (9)$$

We calculate the partial derivatives of the Lagrangian with respect to \mathbf{w} and λ :

$$\frac{\partial}{\partial \mathbf{w}} L(\mathbf{w}, \lambda) = 2\mathbf{A}^T \mathbf{A} \mathbf{w} - \lambda \mathbf{b}, \quad (10)$$

$$\frac{\partial}{\partial \lambda} L(\mathbf{w}, \lambda) = \beta - \mathbf{w}^T \mathbf{b}. \quad (11)$$

A necessary condition for an optimum of this function is $\frac{\partial}{\partial \mathbf{w}} = \mathbf{0}$ and $\frac{\partial}{\partial \lambda} = 0$. Therefore we can use equation 10 to receive:

$$\hat{\mathbf{w}} = (\mathbf{A}^T \mathbf{A})^{-1} \mathbf{b}, \quad (12)$$

where we substituted

$$\frac{2\mathbf{w}}{\lambda} = \hat{\mathbf{w}}. \quad (13)$$

Because λ is still unknown we have determine its value by using equation 11 and substitute again:

$$\lambda = \frac{2\beta}{\hat{\mathbf{w}}^T \mathbf{b}}, \quad (14)$$

finally yielding \mathbf{w} as:

$$\mathbf{w} = \frac{\lambda}{2} \hat{\mathbf{w}} = \frac{\beta}{\hat{\mathbf{w}}^T \mathbf{b}} \hat{\mathbf{w}}. \quad (15)$$

Equation 12 can readily be solved using linear algebra libraries, while equation 15 is a simple scaling. As a default value we choose β and b to be equal to the maximum line integral value of the projection data. This keeps the range of the histogram of the projection images similar. Optimization of this problem is well-posed because it is convex and the data-dependent term is fixed during optimization.

C. Robust estimation

In presence of additional sources of inconsistency, which cannot be reduced using a pixel-wise independent function, degenerate solutions may occur. These degenerate solutions violate the physical model of beam hardening, by introducing reversal points. To deal with this problem, we formulate an additional constraint on our solution to be strictly monotonous. This can be achieved by a positivity constraint on the coefficients:

$$\min(\|\mathbf{A}\mathbf{w}\|_2^2) \quad s.t. : \mathbf{w}^T \mathbf{b} = \beta; \quad w \geq 0 \quad \forall w \in \mathbf{w}. \quad (16)$$

This problem is a quadratic programming problem and cannot be solved linearly. However it is still convex and can be solved using general purpose non-linear optimization methods.

III. EXPERIMENTS

We present three simulation experiments with our method using the robust optimization. In Sect. III-A we evaluate the robustness of our method to image noise. To this end, we use the same model for simulation and restoration to have accurate ground truth. We use the well-known FORBILD phantom, with a polynomial applied to it to simulate the beam hardening effect. Our goal is to retrieve the simulated polynomial.

We proceed by studying the robustness of the proposed algorithm to noise in the geometric description on top of the simulated beam hardening in Sect. III-B.

Because the Epipolar consistency conditions no longer hold in presence of truncation, we study robustness to this kind of corruption in Sect. III-C.

Sect. III-E finally demonstrates an experiment with real data.

A. General feasibility and robustness to noise

We construct the ground truth polynomial from figure 1, to follow our choice of the fixed maximum value of the projections. We proceed by corrupting the projections by applying the inverse of this polynomial. Subsequently we corrupt the projections with poisson-distributed noise. The different noise levels are created by varying the parameter of the Poisson distribution, corresponding to the count of emitted photons[#].

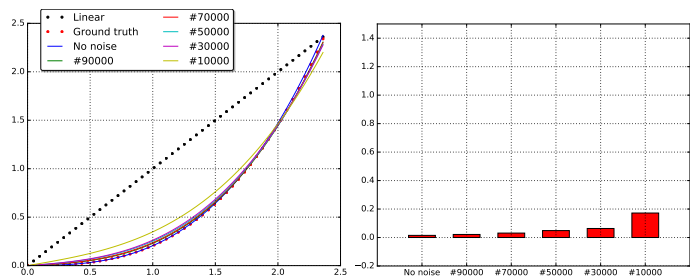


Figure 1: Comparison of results with added noise

From figure 1, an accurate retrieval of the simulated polynomial can be seen in absence of noise. The left figure compares the polynomials visually, the right plot shows the difference in area under the respective polynomials to the area under the ground truth polynomial. Increasing noise degrades the results but even in the presence of severe amounts of noise, beam hardening can be reduced very well. Note that the robustness to noise can be improved further by binning the projections for the intermediate function.

B. Robustness to jitter

To simulate geometric noise, which we refer to as jitter, we use uniformly random distributed noise in u and v direction of the detector coordinates measured in pixels [px]. The same polynomial as in the previous experiment is used. We increase the geometric noise progressively by two pixels. We sum up the result in figure 2.

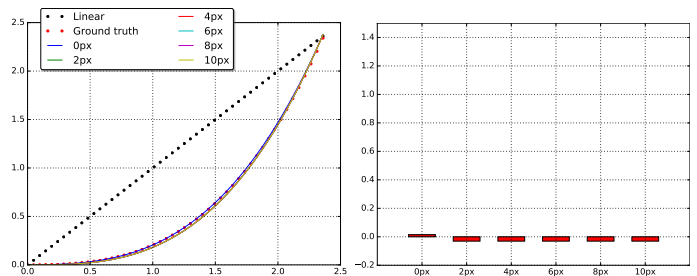


Figure 2: Comparison of results with added geometric noise

We conclude from this experiment that our method shows a quite complicated behaviour in terms of robustness to geometric noise. Since geometric noise can't be accounted for by a pixel-wise transformation the data-term enforces degenerate results. However using our robust estimation we can recover very good solutions even in presence of severe jitter.

C. Robustness to truncation

Truncation is simulated for every direction, by cropping the quadratic image from each of the four sides simultaneously. We apply a symmetric cropping in the image's width and height given as a percentage[%].

	Only	+Noise	+Jitter	+Truncation
SNR Original	11.61	7.46	11.38	5.56
SNR ECC ²	40.16	4.20	20.88	14.25
CNR Original	2.77	1.77	1.40	0.69
CNR ECC ²	28.34	2.80	9.30	8.56

Table I: Quantitative results for the depicted simulations

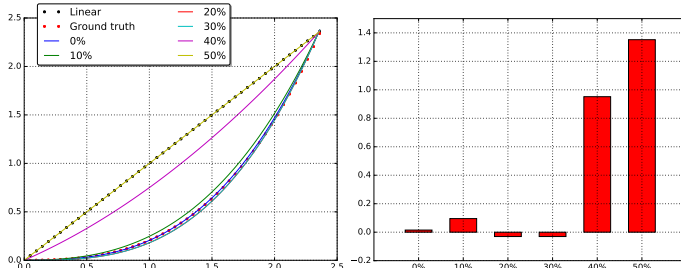


Figure 3: Comparison of results with added truncation

Figure 3 shows our results for this experiment. With increasing truncation, the method tends to produce more linear curves on this object, resulting in a less accurate solution or no reduction at all in case of severe truncation. However the method is robust to truncation in the sense, that our method never degrades the image quality. This can be seen from the polynomials by the fact, that they all represent monotonic convex functions. It can also be seen from the overview figure 4, by the increasing contrast of the truncation example. Note that this image also has to be corrected for truncation artifacts which interacts with the beam hardening effect.

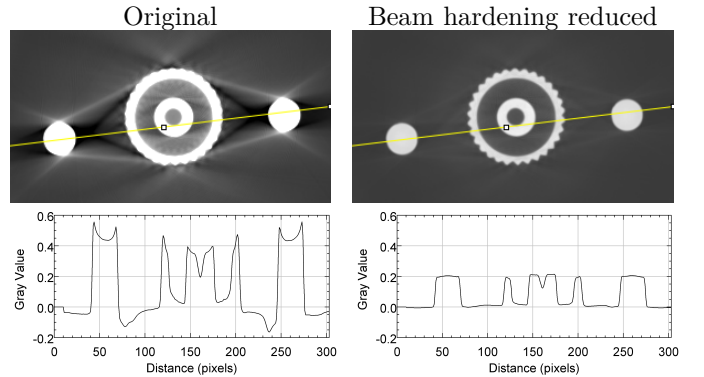
D. Quantitative results

To quantitatively assess the image quality gains using our method we calculate the signal to noise ratio(SNR) as $\frac{\mu}{\sigma}$ over a homogeneous region depicted in figure 5. Because beam hardening is an effect causing structured noise which is not properly reflected by SNR, we additionally report the contrast to noise ratio(CNR). The CNR is calculated as $\frac{|\mu_1 - \mu_2|}{\sigma}$, where μ_1 and μ_2 are regions depicted in figure 5. Our results in table I show that our method increases the SNR for every scenario except the one involving severe image noise. However this does not correspond to a decrease in perceived image quality because the contrast of the image increases greatly. This is reflected in the fact that our method increases the CNR for every single case.

E. Real data experiment

We carry out an experiment on a real object. The object is a metal stopwatch. The effect of beam hardening is reduced using our method. Figure 6 shows an interesting slice of our result. We can see, that the beam hardening effect has been reduced greatly by examining the air between the high density parts. Additionally, the cupping effect is reduced. We measure SNR and CNR in this slice, as 31.81 (SNR) and 31.34 (CNR) for the original data

against 75.09 (SNR) and 71.75 (CNR) after applying our beam hardening reduction algorithm.

Figure 6: Beam hardening reduction on real data. (Grayscale window: C/W = 0.08/0.32 mm⁻¹).

IV. CONCLUSION AND OUTLOOK

We have shown our algorithm to be generally able to reduce the effect of beam hardening without a need for prior knowledge. Furthermore we have shown its robustness to noise, geometric misalignment, truncation and real data. Since the approach by Abdurahman et al. relies on the optimization of the same consistency condition, we expect comparable behaviour to his method. However, our formulation using the linearity of the Radon and the Derivative operators greatly reduces the computational effort of the method, since the Radon transform consumes most of the runtime of the algorithm. In addition, we showed our optimization problem has a unique solution and can readily be solved in closed form.

Our algorithm has the potential to simplify calibration for beam hardening reduction since no prior knowledge about the object, the spectrum or the response characteristics of the detector is required. This is especially convenient for service providers where the precise materials of the scanned object are typically unknown. Future research directions include a more extensive evaluation of the algorithm on real data and an extension to a multi-material method. Also a simultaneous multi-dimensional optimization of geometric and beam hardening parameters promises to provide improved results for both methods.

Acknowledgement

Xiaolin Huang is supported by the Alexander von Humboldt Foundation.

Disclaimer

The concepts and information presented in this paper are based on research and are not commercially available.

REFERENCES

- [1] T. M. Buzug, Ed., *Computed Tomography*. Springer, 2008.
- [2] M. Kachelrieß, K. Sourbelle, and W. A. Kalender, "Empirical cupping correction: A first-order raw data precorrection for cone-beam computed tomography," *Medical Physics*, vol. 33, no. 5, pp. 1269–1274, 2006.

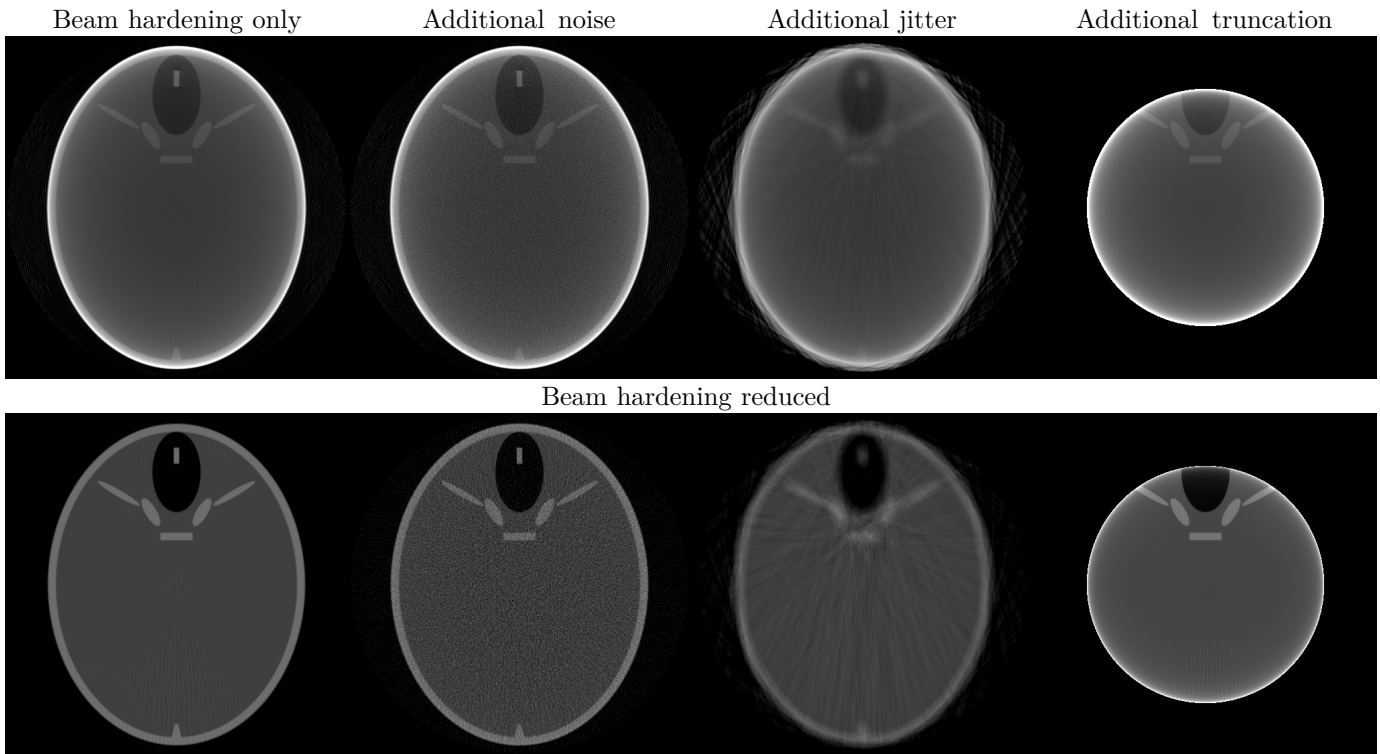


Figure 4: Beam hardening reduction under various additional effects. (Grayscale window: $C/W = 0.02/0.03 \text{ mm}^{-1}$).

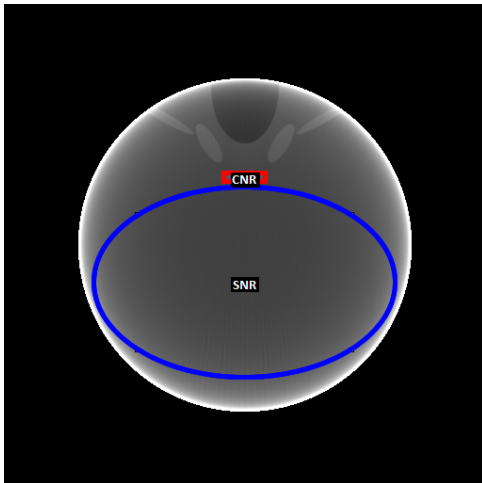


Figure 5: Locations for computation of SNR and CNR

- [3] P. M. Joseph and R. D. Spital, "A method for correcting bone induced artifacts in computed tomography scanners," *Journal Computer Assisted Tomography*, vol. 2, pp. 100–108, 1978.
- [4] M. Wu, Q. Yang, A. K. Maier, and R. Fahrig, "Spectrum binning approach for multi-material beam hardening correction (mmbhc) in ct," in *Proceedings of the third international conference on image formation in x-ray computed tomography*, 2014, pp. 87–90.
- [5] S. Helgason, "Support of radon transforms," *Advances in Mathematics*, vol. 38, no. 1, pp. 91–100, 1980.
- [6] P. R. Edholm, R. M. Lewitt, and B. Lindholm, "Novel properties of the fourier decomposition of the sinogram," *Proceedings SPIE 0671*, pp. 8–18, 1986.
- [7] A. Aichert, M. Berger, J. Wang, N. Maass, A. Doerfler, J. Hornegger, and A. K. Maier, "Epipolar consistency in transmission imaging," *IEEE Transactions on Medical Imaging*, vol. 34, no. 11, pp. 2205–2219, 2015.
- [8] S. Tang, X. Mou, J. Benett, and H. Yu, "Data consistency condition-based beam-hardening correction," *Optical Engineering*, vol. 50, no. 7, 2011.
- [9] S. Abdurahman, R. Frysich, R. Bismarck, M. Friebe, and G. Rose, "Calibration free beam hardening correction using grangeat-based consistency measure," in *Nuclear Science Symposium and Medical Imaging Conference*, 2016.
- [10] P. Grangeat, "Mathematical framework of cone beam 3d reconstruction via the first derivative of the radon transform," *Lecture Notes in Mathematics*, vol. 1497, pp. 66–97, 1991.
- [11] C. Debbeler, N. Maass, M. Elter, F. Dennerlein, and T. M. Buzug, "A new ct rawdata redundancy measure applied to automated misalignment correction," in *Fully Three-Dimensional Image Reconstruction in Radiology and Nuclear Medicine*, 2013, pp. 264–267.